Published in final edited form as:
Immunity. 2008 December ; 29(6): 888–898. doi:10.1016/j.immuni.2008.10.008.

PlexinD1 controls migration of positively-selected thymocytes into the medulla

Young I. Choi[1,2], **Jonathan S. Duke-Cohan**[1,2], **Wesam B. Ahmed**[1], **Maris A. Handley**[1], **Fanny Mann**[3], **Jonathan A. Epstein**[4], **Linda K. Clayton**[1,2], and **Ellis L. Reinherz**[1,2,*]

1 *Laboratory of Immunobiology, Department of Medical Oncology, Dana-Farber Cancer Institute, Boston, MA 02115, USA*

2 *Department of Medicine, Harvard Medical School, Boston, MA 02115, USA*

3 *Developmental Biology, Institute of Marseille Luminy, CNRS UMR 6216, University of Mediterranee, Case 907, Parc Scientifique de Luminy, 13288 Marseille Cedex 09, France*

4 *Department of Cell and Developmental Biology and the Cardiovascular Institute, University of Pennsylvania, Philadelphia, PA 19104, USA*

Summary

Precise intrathymic cell migration is important for thymocyte maturation and architecture. The orchestration of thymocyte trafficking, however, is not well understood at a molecular level. Here, we describe highly-regulated plexinD1 expression on $CD4^+CD8^+$ double positive (DP) thymocytes which is further affected by T cell receptor/co-receptor engagement. Activation of plexinD1 via one of its ligands, semaphorin3E, represses CCR9/CCL25 signaling in $CD69^+$ thymocytes. In the absence of plexinD1, $CD69^+$ thymocytes remain in the cortex, maturing to form ectopic SP thymocyte clusters in *Plxnd1*-deficient fetal liver cell-transplanted mice. As a consequence, the boundary between DP and SP thymocytes at corticomedullary junctions is disrupted and medullary structures form under the thymic capsule. These results demonstrate the importance of plexinD1 in directing migration of maturing thymocytes via modulation of biological responses to chemokine gradients.

Introduction

Thymic ontogeny is a finely coordinated multi-step process involving maturation of incoming bone marrow-derived precursors into immunocompetent T lymphoid cells. A complex set of interactions drives this progression including bidirectional signaling between developing thymocytes and thymic epithelial cells (TEC) along with cues from chemokine gradients (Anderson and Jenkinson, 2001). The thymic capsule and TEC precursors originate from a single third pharyngeal pouch after its disconnection from the third cleft ectoderm (Rodewald, 2008). Thymic organogenesis begins upon thymocyte precursor migration to the thymic anlage. As incoming thymocytes pass through the initial stages of differentiation, they are first classified as double negative (DN) by the lack of expression of CD4 and CD8 and further characterized by the expression of CD44 and CD25. These immature DN thymocytes induce the development of thymic corticomedullary structures by affecting the development and

*Address correspondence to: Ellis L. Reinherz, M.D., Dana-Farber Cancer Institute, 77 Avenue Louis Pasteur, HIM 418, Boston, MA 02115; Tel: 617-632-3412; Fax: 617-632-3351; ellis_reinherz@dfci.harvard.edu.

proliferation of cortical epithelial cells (cTEC) or medullary epithelial cells (mTEC) (Rossi *et al.*, 2006). Cortical structure is disorganized in the thymus of *hCD3ε* tg mice where T cell development is blocked at the CDD44^{+}CD25^{-} DN1 stage but cortical structure is well organized in RAG2$^{-/-}$ mice where T cell development is blocked at the CD44^{-}CD25^{+} DN3 stage, suggesting that CD4^{-}CD8^{-} thymocytes expressing CD44 and CD25 (DN2) are required for well-organized corticomedullary structure (Klug et al., 1998). In addition, there is evidence that mTEC development and proliferation require CD4^{+} or CD8^{+} single positive (SP) thymocytes: mTEC do not develop in mice lacking mature T cells, (Shores *et al.*, 1994) whereas transplanted mature SP T cells induce a thymic medullary structure in SCID mice (Surh *et al.*, 1992). These results suggest that the distribution of maturing thymocyte subpopulations may affect thymic architecture and that analysis of the intrathymic migration of hematopoietic and epithelial components is important in understanding thymic organogenesis.

Thymocyte subpopulations express distinct chemokine receptor patterns, in part mandating their differential intrathymic migration patterns (Ansel and Cyster, 2001). For example, DN1 cells migrate to the thymic capsule in response to CXCR4 ligand (CXCL12/SDF1) produced by the thymic cortex (Plotkin *et al.*, 2003). The CD44^{+}CD25^{int}CD4^{-}CD8^{-} (DN1-2 intermediate) cells respond to CCR7 ligands (CCL19/MIP3β and CCL21/6Ckine; CCL19/21) fostering migration to and retention in the subcapsular zone (Misslitz *et al.*, 2004). Although resting CD4^{+}CD8^{+} double positive (DP) thymocytes are CCR9^{+}, they do not respond to CCR9 ligand (CCL25; TECK); however, activated DP thymocytes expressing both CCR9 and CCR7 respond to CCL25 and CCL19/21. Mature CD4^{+}CD8^{-} or CD4^{-}CD8^{+} single positive (SP) thymocytes respond to CCL19/21 and migrate to the medulla where tissue-specific self-peptide/MHC complexes are provided to the maturing thymocytes, further facilitating removal of potentially autoreactive T cells (Ueno *et al.*, 2004).

It is clear that there are significant gaps in our current understanding of the signals mediated by chemokines and their receptors during thymic development. For example, CCL19/21 effects are pleiotropic, directing DN1-2 intermediate thymocytes to move to the subcapsullary zone, transitioning DP/SP thymocytes to move to the medulla, and mature SP thymocytes to exit the thymus (Ueno *et al.*, 2002; Misslitz *et al.*, 2004; Ueno *et al.*, 2004). Furthermore, activated DP thymocytes respond to CCL25 expressed in the cortex and to CCL19/21 expressed in the medulla. Interestingly, CCL25 is provided by the cTEC (Wurbel *et al.*, 2000) whereas CCL19/21 are expressed both in the medulla and the thymic capsule (Misslitz *et al.*, 2004; Ueno *et al.*, 2004). During positive selection, the maturing thymocytes are capable of receiving both signals because activated CD69^{+} DP thymocytes express CCR7 and CCR9. Nevertheless, after positive selection, these thymocytes migrate rapidly to the medulla, despite the CCL25 cortical gradient (Uehara 2002). Therefore, a fundamental issue is to understand how activated thymocytes repress CCR9 signaling to allow their efficient CCR7-mediated migration to the medulla. As these complex chemokine networks suggest the existence of additional molecular pathways that regulate intrathymic migration of DP and SP thymocytes, we examined the global gene expression patterns of sorted developing thymocytes in order to identify such thymocyte subset-restricted molecules. We found that *Plxnd1* mRNA is highly expressed in DP thymocytes and rapidly repressed thereafter. Recently, plexinD1 together with its ligand, semaphorin 3E (sema3E), was shown to play a critical role in directing angiogenesis (Kruger *et al.*, 2005). *Plxnd1* deficiency results in defective developmental separation of the aorta and the pulmonary artery as well as inappropriate infiltration of blood vessels into somites during embryogenesis (Gitler *et al.*, 2004; Gu *et al.*, 2005). Given the precisely-regulated expression of *Plxnd1* in thymocytes, we hypothesized that the directional control exerted by other plexins and semaphorins during neuronal axon pathfinding (Kruger *et al.*, 2005) and by PlexinD1 in angiogenesis (Gitler *et al.*, 2004; Gu *et al.*, 2005) is exploited for control of thymocyte migration during thymic development. The *in vitro* and *in vivo* studies presented herein show, for the first time, that this is the case.

Results

Global gene expression analysis with DP, CD8 intermediate and CD8 SP thymocytes

To identify genes differentially expressed during positive selection, global gene expression patterns were analyzed using sorted DP, CD8 intermediate and CD8 SP thymocytes from 5–6 week old homozygous *N15TCR* $tg^{+/+}$ $RAG2^{-/-}$ $H2^b$ mice (Fig 1A). This TCR is specific for the immunodominant nucleoprotein octapeptide (VSV8) bound to $H\text{-}2K^b$ (Shibata *et al.*, 1992). Hence, on the $RAG2^{-/-}$ background, no CD4 SP thymocytes are generated (Ghendler *et al*., 1997). Fig. 1B represents the hierarchal clustering of those genes among the 45,102 assayed whose alteration showed a lower confidence bound (LCB) value >2.0 in two independent samples of *N15TCRtg*$^{+/+}$ $RAG\text{-}2^{-/-}$ $H2^b$ DP, CD8 intermediate and CD8 SP thymocytes.

Four patterns of gene expression were evident with patterns I (induction) and II (repression) much more frequent than patterns III and IV (Fig. 1B and C and Fig. S1), which exhibited differential expression of genes in the CD8 intermediate subset (Fig. S1). In pattern I, the expression of genes was low in DP thymocytes and increased successively in the intermediate and CD8 SP thymocytes (Fig. 1B and C). Among the greatest gene induction is that of αE integrin (CD103), undergoing a 42-fold change (FC) (LCB=22.52) from DP to CD8 SP thymocytes. Interestingly, human mTEC were recently shown to express E-cadherins, the ligand for the αE (CD103) β7 integrin (Kutlesa *et al.*, 2002). These findings provide one of several independent validations of our current expression array data. Also upregulated is CD94 (the killer cell lectin-like receptor subfamily D member 1) which forms CD94/NKG2 heterodimers and belongs to the group of C-type lectins expressed on ~50% of splenic NK cells and a subset of CD8 T cells, binding to Qa1 in mice and its human homologue, HLA-E in human (Vance *et al*., 1998). Apoptosis in CD8 T cells and NK cells themselves is inversely related to CD94 expression, suggesting that CD94 plays an important role in maintenance of CD8 T cells. Not surprisingly, other genes such as *Schlafen-1* involved in growth regulation are upregulated as well (Schwarz *et al*., 1998).

Pattern II consists of genes whose expression is reduced during successive maturation. RAG-1 is reduced 13.3-fold as expected since TCR rearrangements are completed during the DP thymocyte stage (Turka *et al.*, 1991). *RORγ*, a T lineage specific isoform of ROR, found only in immature DP thymocytes and important in their survival of DP thymocytes (Sun *et al*., 2000) shows an 11.4-fold decrease during the DP to CD8SP transition. The reduction of *Glucocorticoid(GC)-induced transcript 1* with maturation correlates with the increased GC resistance of mature thymocytes (Reichardt *et al*., 1998). Although not shown, *CD4* gene expression undergoes the greatest reduction during the DP to SP thymocyte transition with levels falling 433-fold (LCB = −9.86). *Plxnd1* gene expression is also dramatically repressed during the DP to CD8 SP thymocyte transition, exhibiting a 96-fold decrease (LCB = −10.63). PlexinD1 is a large (~200Kd) transmembrane glycoprotein and is a recent addition to the plexin family, other members of which are associated with neuronal axon pathfinding. A recent elegant report identified sema3E as a functional ligand for plexinD1 (Gitler *et al*. 2004). Sema3E is a secreted protein and induces a repulsive signal on $plexinD1^+$ endothelial cells to prevent blood vessel formation (Gu *et al*., 2005). The identification of plexinD1 in directing endothelial cell migration and developmental angiogenesis led us to analyze the relationship between plexinD1 and intrathymic migration.

PlexinD1 is highly expressed in DP thymocytes

In situ hybridization with antisense *Plxnd1* cRNA showed *Plxnd1* expression in *N15TCRtg*$^{+/+}$ $RAG\text{-}2^{-/-}$ and B6 thymi in many cortical thymocytes but not medullary thymocytes (Fig. S2), consistent with our expression array results. In addition, rabbit antisera

(anti-plexinD1 IC) raised against a cytoplasmic plexinD1 peptide (LEEQAEKRGISDPD) specifically react with a protein band of ~220Kd in thymocyte lysates and can be absorbed with the immunizing peptide but not a control peptide (Fig. 2A). The same size band is identified in human *Plxnd1*-transfected 293T cells and murine thymocytes (Fig. 2B). Moreover, immunohistological staining of B6 thymus with an ectodomain peptide-specific Ab (anti-plexinD1 EC) and our anti-plexinD1 IC (C4992) shows staining of similar intensity in cortex but a virtual absence of medullary staining (Fig. 2C).

Within the hematopoietic system, plexinD1 protein expression is largely, if not exclusively, restricted to thymocytes and absent from bone marrow cells, lymph node cells and splenocytes (Fig. 2D). Real time PCR analysis shows strong *Plxnd1* expression in DP thymocytes but not in DN thymocytes or CD8 SP thymocytes while low expression is observed in CD4 SP thymocytes (Fig. 2E). Repression of *Plxnd1* mRNA in mature SP thymocytes suggests that TCR signaling may be involved in the regulation of plexinD1 expression. Costimulation of total thymocytes with anti-CD3 and anti-CD8α or anti-CD4 mAbs represses plexinD1 expression over time (Fig. 2F lower panels). Stimulation of total thymocytes, however, with anti-CD3 antibody alone did not reduce plexinD1 expression (Fig. 2F upper left panel) although CD69 expression was induced to similar levels in all stimulation conditions (data not shown). Anti-CD3 plus anti-CD28 mAb stimulation modestly reduced plexinD1 protein on western blot analysis (Fig. 2F upper right panel). Quantitative densitometry of this experiment (Fig. 2F right graph) shows that CD4 or CD8 coreceptor crosslinking in conjunction with anti-CD3 mAb is important in downregulating plexinD1 protein expression. The data lead to the proposal that conjoint TCR and co-receptor stimulation by peptide/MHC may modify the migratory potential of thymocytes through modulation of expression of plexinD1, altering the response to directional cues from sema3E or other potential ligands. Subsequent experiments were aimed at testing this notion.

Purified semaphorin3E binds to plexinD1 on thymocytes

Given that, to date, sema3E is the main known ligand for plexinD1, we examined whether this specific interaction affected thymocyte migration and differentiation. For this purpose, we produced sema3E and the ectodomain of mouse plexinD1 as C-terminal Fc-fusion constructs (termed sema3E-Fc and plexinD1-Fc, respectively). PlexinD1-Fc purity was assessed as ≥95% by Coomassie blue gel staining after S200 gel filtration (Fig. 3A insert). Sema3E and sema3F (a negative control protein) contain a furin cleavage site between the sema and the Fc domains. The intact fusion proteins run at ~125Kd but cleavage at the furin site liberates an 80Kd stalk/Fc fusion fragment, most evident in the sema3E-Fc protein lane. The lower band does not bind plexinD1 (Fig. 3B). The binding as observed in SPR analysis yielded an apparent ^{K}D for the plexinD1-sema3E interaction of 43.4nM (Fig. 3A). Sema3E but not sema3F demonstrates the capacity to bind plexinD1. To confirm the interaction using a second method, we immobilized plexinD1 ectodomain on beads and tested its efficacy at pulling down sema3E-Fc protein. By Coomassie blue gel staining, sema3E-Fc was clearly bound to beads crosslinked with plexinD1-Fc but not to control beads (Fig. 3B) and no binding was observed using sema3F-Fc. Testing sema3E binding to plexinD1 on thymocytes, we find that DP thymocytes ($CD69^-$ or $CD69^+$) and $CD69^+$ CD4 SP thymocytes show strong binding, $CD69^+$ CD8 SP thymocytes show intermediate binding and DN and $CD69^-$ SP thymocytes show minimal binding (Fig. 3C). Thus, DP thymocytes and $CD69^+$ maturing thymocytes express surface plexinD1 able to bind sema3E. Since sema3E is the only known ligand for plexinD1, it was critical to establish not only that sema3E is expressed in the thymus but also its spatial expression before any model of plexinD1 influence on thymocyte migration can be formulated. The very low levels of sema3E expressed in thymus together with poor availability of high quality anti-sema3E antibody reagents hamper such analysis at the protein level. Nevertheless, clear detection of *Sema3e* transcript in thymic total RNA by RT-PCR led us to analyze thymic

regional *Sema3e* transcript expression using Laser Capture Microdissection (LCM). *Sema3e* is expressed very highly in the medulla in comparison to the corticomedullary junction, cortex and subcapsullary zone (Fig. 3D) and sema3e expression levels correlate reciprocally with those of the PlexinD1 transcript (Fig. 2E and S2). These results suggested that soluble sema3E protein may form a gradient from the medulla to the thymic capsule and regulate migration of plexinD1^{+} thymocytes.

Sema3E inhibits CCR9-mediated CD69^{+} DP thymocyte migration

Based on its established role in guiding vessel directionality during angiogenesis (Gu *et al*., 2005), we speculated that plexinD1 may function in controlling thymocyte migration during the DP to SP transition. To test this notion, we developed a transwell-based migration assay. Sema3E-Fc alone had no effect on thymocyte migration, suggesting that the sema3E-plexinD1 interaction does not directly induce a change in migratory pattern, perhaps due to a requirement for more than one ligand-receptor interaction (data not shown). Accordingly, we examined whether sema3E would inhibit CCR9 and CCR7 chemokine-mediated migration of thymocytes responding *in vitro* to the ligands CCL25 and CCL19/21, respectively (Fig. 4A). It is known that CCL25 induces migration of activated CD69^{+} DP thymocytes to cTEC (Campbell *et al*., 1999; Wurbel *et al*., 2000). The majority of DP thymocytes express CCR9 but in the resting state do not respond efficiently to the CCL25 ligand expressed in the cortex. On the other hand, CCL19/21 induces migration of activated CCR7-bearing CD69^{+} DP thymocytes as well as mature SP thymocytes to the medulla. Fig. 4B shows that, in the transwell migration assay, CCL25 induced the migration of CD69^{+} TCR^{high} DP thymocytes whereas CCL21 primarily induced mature CD4 SP thymocyte migration. The effect of sema3E-Fc was specific, inhibiting CCR9-mediated total CD69^{+} thymocyte migration efficiently but having only a weak effect upon CCR7-mediated migration (Fig. 4B and C). Although not shown, no effect on migration by CCL21 or CCL25 was observed either with sema3F-Fc or Fc protein alone.

While both CD69^{+} and CD69^{-} DP thymocytes express high levels of CCR9 (Fig. 4D), CD69^{-} DP thymocytes did not migrate in the *in vitro* transwell assay, suggesting that TCR stimulation may alter intracellular signaling pathways making cells competent to respond to migrational cues. In support of other signaling pathways contributing to thymocyte migration (Swainson et al., 2005), we found that both CD69$^{-/-}$ and CD69$^{+/+}$ TcRlow DP thymocytes could migrate in response to CXCL12 in the transwell assay, presumably binding to CXCR4 widely-expressed in the thymus (Fig. S3). Further, this response could be efficiently inhibited by sema3E but not by the related sema3F, supporting involvement of thymocyte-expressed plexinD1 in modifying signaling cues for migration. Comparison of our results suggests that CCL25 induction of CCR9 signaling may be more sensitive to inhibition by sema3E than CXCL12 induction of CXCR4 signaling (data not shown).

On the other hand, CCL21-mediated migration directly correlates with CCR7 expression levels, consistent with earlier studies of DP thymocytes in CCR7 transgenic mice, implying that CCR7 signals are not dependent on TCR stimulation (Kwan and Killeen, 2004) and CCR7 uses different signaling molecules to CCR9 or CXCR4. Interestingly, CD69^{-} CD4 SP thymocytes express high CCR7 but no CCR9 while CD69^{-} CD8 SP thymocytes express low levels of both CCR7 and CCR9 (Fig. 4D). Hence, CD69^{-} CD8 SP and CD69^{-} CD4 SP thymocytes may respond differently to the surrounding chemokine environment.

Intrathymic localization of activated CD69^{+} TCR^{high} thymocytes

Since sema3E-Fc inhibited CCL25-mediated migration of CD69^{+}TCR^{high} thymocytes but not CCL21-mediated migration, we evaluated whether plexinD1 deficiency might affect the chemokine responsiveness of CD69^{+} TCR^{high} thymocytes, altering their distribution in the thymus. To this end, we examined *Plxnd1*$^{-/-}$ embryos. Sections of 14.5 dpc embryos showed

that the *Plxnd1*$^{-/-}$ thymus was disorganized compared to the wild type control embryonic thymus, with no clear cortical/medullary demarcation (Fig. S4). These findings suggest that plexinD1 expression is necessary for establishment of a normal thymic architecture. PlexinD1 expression is also essential for normal vasculature development (Gu *et al*., 2005) and the *Plxnd1*$^{-/-}$ embryos were smaller than wild type controls and had the truncus artery as reported (Gitler *et al*., 2004). Furthermore, *Plxnd1*$^{-/-}$ embryos (18.5 dpc) had two separated thymic lobes in the subclavian region whereas wild type controls had a single fused thymus above the heart (Fig. S5). These results were observed in all *Plxnd1*$^{-/-}$ embryos analyzed at this age (more than 20 embryos) as well as neonatal *Plxnd1*$^{-/-}$ mice.

To exclude that this thymic phenotype was simply a consequence of vascular alteration or developmental retardation, we performed fetal liver cell transplantation transferring Ly5.2^{+} *Plxnd1*$^{-/-}$ or *Plxnd1*$^{+/+}$ fetal liver cells into irradiated Ly5.1^{+} C57BL/6 congenic mice. In this instance, the recipient thymic infrastructure is normal so that the influence of plexinD1 on thymocyte development can be followed. T cell development was analyzed 4–5 weeks after reconstitution. To confirm the reconstituting genotype, thymocytes were stained first with sema3E-Fc. Sema3E-Fc bound to Ly5.2^{+} *Plxnd1*$^{+}$ fetal liver-derived DP and CD4 SP thymocytes in a fashion similar to the corresponding thymocytes of wild-type C57BL/6 mice. In contrast, and as expected, sema3E-Fc did not bind to Ly5.2^{+} *Plxnd1*$^{-/-}$ fetal liver-derived DP and CD4 SP thymocytes (Fig. S6C). We thus conclude that plexinD1 is the only surface receptor on thymocytes capable of detectable interaction with sema3E. Analysis of Ly5.2^{+} thymocytes, lymph node cells and splenocytes with anti-CD4/CD8/TCRβ/Ly5.2/B220 mAbs yielded similar results for *Plxnd1*$^{-/-}$ and *Plxnd1*$^{+/+}$ reconstituted animals (Fig. S6A and B). Likewise, other cell surface markers including CD2/CD5/CD44/CD25 revealed no differences between Ly5.2^{+} *Plxnd1*$^{-/-}$ and Ly5.2^{+} *Plxnd1*$^{+/+}$ thymocytes (data not shown).

In thymic cryosections of fetal liver cell transplanted mice stained with anti-CD4/CD8/CD69 mAbs, the CD69^{+} *Plxnd1*$^{+/+}$ thymocytes, like those of normal B6 mice, localized inside the medulla or adjacent to the corticomedullary junction. On the other hand, the majority of CD69^{+} *Plxnd1*$^{-/-}$ thymocytes were found outside the medulla with very few CD69^{+} *Plxnd1*$^{-/-}$ thymocytes within the medulla, implying that plexinD1 is important in directed migration of activated thymocytes (Fig. 5A). To examine the effect of those CD69^{+} *Plxnd1*$^{-/-}$ thymocytes on thymic architecture, we analyzed the SP thymocyte distribution in the thymic cortex. Retarded migration of activated DP thymocytes might lead to an increase in cortex-localized SP thymocytes. To this end, thymic cryosections were stained with anti-CD4, anti-CD8α and ER-TR5, a marker of thymic medullary eptithelium. Then, cortex-localized SP thymocytes were enumerated. In magnified images, *Plxnd1*$^{+/+}$ SP thymocytes in the cortex were primarily single cells while large SP thymocyte clusters colocalized with the medulla-specific ER-TR5 staining (Fig. 5B and Fig. S7A left panel merged image). In contrast, *Plxnd1*$^{-/-}$ SP thymocytes localized in the cortex were found as SP thymocyte clusters and did not colocalize with medullary ER-TR5 stained areas (Fig. 5B and Fig. S7A right panel merged image). This microscopic observation was supported by quantitative analysis of SP thymocyte cell cluster size in the cortex (Fig. 5B).

Ectopic medulla formation in Plxnd1$^{-/-}$ fetal liver cell transplanted mice

It has been reported that SP thymocytes or activated thymocytes can induce thymic medulla formation in a thymus without a preexisting medulla (Surh *et al*., 1992; Shores *et al*., 1994). It therefore follows that abnormal accumulation of such cells in a thymic cortex may influence medullary formation. In ~90% *Plxnd1*$^{-/-}$ fetal liver cell transplanted mice, the corticomedullary boundary separating DP from SP cells was disrupted. In contrast, in B6 or *Plxnd1*$^{+}$ fetal liver cell transplanted mice, there was a normal, well-demarcated alignment of SP thymocytes in the medulla and DP thymocytes in cortex (Fig. S7B). Small ER-TR5+

microscopic medullary structures were found to be connected directly to the thymic capsule in >90% of *Plxnd1*$^{-/-}$ fetal liver cell transplanted mice (Fig. S8) with large subcapsular medulla-like structures observed in approximately one-third of the same mice (Fig. 5C).

Localization of activated CD69^{+} TCR^{high} thymocytes in Sema3e$^{-/-}$ mice

Based on the well-established interaction of plexinD1 with sema3E, we analyzed whether *Sema3e* deficiency induces a similar defect in CD69^{+} thymocyte migration and modifications of thymic cellular organization. In thymic cryosections stained with anti CD4/CD8α/CD69 mAbs, the CD69^{+} thymocytes from *Sema3e*$^{+/+}$ mice localized inside the medulla or adjacent to the corticomedullary junction. In contrast, the majority of CD69^{+} thymocytes from *Sema3e*$^{-/-}$ mice were found outside the medulla, implying that sema3E is also important in directed migration of activated thymocytes (Fig. 6A). Analysis of the overall thymic structure of *Sema3e*$^{-/-}$ mice by histology and anti-keratin8/ER-TR5 mAbs reveals an even greater disturbance of cortical and medullary organization than that observed in *Plxnd1*$^{-/-}$ fetal liver cell transplanted thymi. ER-TR5^{+} regions are observed under the thymic capsule and colocalized with DP cell regions, identified by CD4/CD8 staining of adjacent sections, whereas there is a clear delineation of cortex and medulla corresponding to DP and SP cell localization, respectively, in *Sema3e*$^{+/+}$ thymi. Histological examination of thymi from *Sema3e*$^{-/-}$ mice further confirmed the lack of a clear delineation of the corticomedullary junction (Fig. 6B and S9B).

Discussion

We show that plexinD1-sema3E interaction regulates the CCR9 signals in activated CD69^{+} DP thymocytes such that these post-selection cells are induced to migrate to the medulla. As a consequence, in *Plxnd1*$^{-/-}$ fetal liver cell transplanted mice or in *Sema3e*$^{-/-}$ knockout mice, there is an aberrant accumulation of CD69^{+} thymocytes including SP thymocytes in the cortex. Formation of an abnormal medulla from atopic localization of these mature thymocytes is observed within the cortex consistent with the finding that these cells are known to induce mTEC differentiation (Surh *et al*., 1992). Our results clearly show that plexinD1 and sema3E are important in the directed migration of maturing thymocytes and in the orderly formation of a well-demarcated thymic corticomedullary structure. TCR triggering via positive selection at the DP thymocyte stage stimulates a differentiation process that is synchronized with directed cell migration such that mature SP thymocytes are normally localized in the medulla. This process is uncoupled by disruption of *Plxnd1* or *Sema3e*. SP thymocyte development can occur in mice whose thymus lacks a medulla as a result of a defective lymphotoxin beta signaling pathway (DeKoning *et al*., 1997; Elewaut and Ware, 2007). These data are in agreement with our finding that a thymic cortex can support SP thymocyte development therein.

The plexins encode large (~200Kd) transmembrane glycoproteins with some domain similarity to the scatter factor receptors encoded by the MET gene family and RON receptor tyrosine kinases (Kruger *et al*., 2005). There are four plexin families (PLXN-A, -B, -C, -D) which function as receptors for multiple subfamilies of semaphorins, sometimes in the context of neuropilin-1 and neuropilin-2, to control cell dissociation and repulsion in a variety of tissue types. About 20 vertebrate semaphorins are known, classified in 5 distinct subfamilies (Kruger *et al*., 2005). In the nervous system, the effects of secreted semaphorin-plexin interaction on axonal pathfinding are generally repulsive (Kruger *et al*., 2005). The cytoplasmic domain of each plexin contains a GTPase activation domain (GAP) of ~600aa encompassing a central Rac/Rho-like binding motif (Suzuki *et al*., 2008). This domain binds Rnd1 which may disrupt intrinsic GAP structure, thus fostering the increased self-directed GTPase activity of R-Ras, in turn leading to less integrin-mediated adhesion to the extracellular matrix (ECM) (Suzuki

et al., 2008). PlexinD1 may regulate the migration of activated thymocytes in a similar way by regulating integrin or other cell adhesion molecule-mediated adhesion (Fig 7A).

Defective migration of maturing thymocytes into the medulla has been observed to lead to the failure of central tolerance. In $CCR7^{-/-}$ mice, for example, an increase in the number of SP cells in the thymic cortex is associated with autoimmune phenomena, a pathology attributed to the loss of CCR7-directed migration of maturing thymocytes to the medulla (Ueno *et al*., 2004; Kurobe *et al*., 2006). These results suggest that *Plxnd1*$^{-/-}$ fetal liver cell transplanted mice may foster autoimmune disease, perhaps due to an increased survival of autoreactive thymocytes. However, as mature $CD4^+$ SP thymocytes express CCR7 but not CCR9 (Fig. 4D), $CD4^+$ SP thymocytes should still be able to migrate to the medulla even in *Plxnd1*$^{-/-}$ fetal liver cell transplanted mice. In contrast, in $CCR7^{-/-}$ or its ligand-deficient mice, SP thymocytes do not migrate to the medulla, resulting in small and fragmented medullary structures (Misslitz *et al*., 2004; Ueno *et al*., 2004). Thus, *Plxnd1*$^{-/-}$ and *Sema3e*$^{-/-}$ mice present a thymic organization and phenotype similar to that of $CCR7^{-/-}$ mice. We expect, however, that any autoimmune disease phenotype may be milder in *Plxnd1*$^{-/-}$ fetal liver cell transplanted mice or *Sema3e*$^{-/-}$ mice compared to $CCR7^{-/-}$ mice.

The relative localization of DP and SP thymocytes is important in the formation of thymic corticomedullary structures. For example, analysis of CCR7 transgenic mice revealed abnormal migration of immature DP thymocytes into the medulla with attendant disruption of normal thymic architecture (Kwan and Killeen, 2004). It is currently unclear which signals normally exclude DP thymocytes from the medulla. The reciprocal expression pattern of plexinD1 on DP cells and sema3E in the medulla suggests that the expression of plexinD1 results in repulsion away from the sema3E gradient, as is seen in mammalian cortical brain development (Watakabe *et al*., 2006), and that downregulation of plexinD1 during the DP to SP transition breaks down the repulsion and allows the cells to respond to the CCL21 gradient attracting cells to the medulla. The absence of plexinD1 would then be predicted to disrupt all stages of DP cell migration (as we observe). This hypothesis also predicts the disorder found in mice lacking sema3E (Fig S7, S8 and S9). Whereas the localization of DP and SP thymocytes is regulated by chemokines according to specific spatial and temporal patterns in the thymus, DP and SP thymocytes also regulate the development of cortex and medulla, showing that thymocytes and thymic epithelial structures develop in a co-dependent fashion. Such thymocyte-epithelium crosstalk has been documented (Lerner *et al*., 1996).

TCR signaling in thymocytes is an important regulator of both CCR9 expression and CCR9-mediated migration. After pre-TCR complex signaling, DN thymocytes initiate CCR9 expression but display weak responsiveness to CCL25 in an *in vitro* transwell migration assay (Norment *et al*., 2000). Following TCR stimulation, activated DP thymocytes strongly respond to CCL25 expressed by cTEC (Wurbel *et al*., 2000). It is unclear why CCL25 does not induce rapid migration of unstimulated DP thymocytes expressing high levels of CCR9, but this observation is consistent with the slow movement of cortical thymocytes observed using two-photon microscopy (Ladi *et al*., 2006). TCR signaling may alter the cytoskeletal network to regulate productive CCR9-driven motility. Since plexinD1 alone does not induce thymocyte migration but rather inhibits CCR9-mediated migration of activated DP thymocytes, plexinD1 may block migration by disrupting the cytoskeleton-integrin network (Kruger *et al*., 2005).

While CCR9 is important for T-lymphoid progenitor cell migration to fetal thymus prior to vascularization (Liu *et al*., 2006), the function of CCR9 in thymocytes is not well-established (Uehara *et al*., 2002). Because CCL25 is expressed not only in cTEC but also in $CD11b^-$ thymic dendritic cells (DC) (Vicari *et al*., 1997), CCR9 activation may enhance TEC-thymocyte or DC-thymocyte interactions for positive and negative selection.

To date, the only clearly defined ligand of plexinD1 is sema3E, although one recent report suggests that sema4A may also be a ligand (Toyofuku *et al*., 2007). We have constructed both sema3E-Fc and sema4A-Fc chimeric proteins, however, and observed nanomolar binding of the former but no detectable binding of the latter (Fig. S10).

In general, it is becoming increasingly appreciated that the semaphorin/plexin axis associated with axon pathfinding also plays a role in lymphocyte development and function. For example, semaphorin4A binds to Tim2, an interaction important both in T cell priming and development of a Th1 immune response (Suzuki *et al*., 2008). Semaphorin7A binds to $\alpha_1\beta_1$ integrin where this interaction is important in T cell-mediated hypersensitivity (Suzuki *et al*., 2008). Semaphorin4D binds to CD72 on B cells and this interaction is significant in the CD40-induced B cell response and $CD5^+$ B-1 cell development (Suzuki *et al*., 2008). PlexinA4 on T cells functions in the inhibition of T cell proliferation and activation, leading to development of severe autoimmune disease in *Plxna4* deficient mice (Yamamoto *et al*., 2008). PlexinA1 forms a protein complex with Trem2 and DAP12 and binds to semaphorin6D. In *Plxna1* deficient mice, DCs do not stimulate antigen-specific T cells efficiently and osteopetrosis develops due to a T cell-dependent defect in osteoclast development (Suzuki *et al*., 2008). These earlier results show that the semaphorin/plexin receptor-ligand pairs have pleiotropic functionality in the mature peripheral immune system. Our current results examining plexinD1 and sema3E extend the role of the plexin/semaphorin axis to the developing T lineage and suggest that in all likelihood, other plexins and semaphorins further contribute to the fine positional coordination and migratory paths of cells within the thymus.

Experimental Procedures

Antibodies and reagents

Anti-FcγR (2.4G2), anti-TCRβ-APC, anti-CD69-FITC, anti-CD25-PE, anti-CD44-biotin, streptavidin-APC-Cy7, anti-CD4-Alexaflour647 and anti-Ly-CD45.2-FITC were purchased from BD-Pharmingen (San Jose, CA). Anti-CD4-Pacific Blue and anti-CD8α-Pacific Orange were purchased from Calbiochem (San Diego, CA). TROMA1 (anti Keratin8 mAb) clone was purchased from Developmental Studies Hybridoma Bank (Iowa City, IA). ER-TR5 was provided by Dr. W. van Ewijk (Leiden University Medical Center, Netherlands). Unconjugated and HRP-conjugated F(ab') anti-mouse γ_{2c} heavy chain was purchased from Jackson Immunoresearch (West Grove, PA).

Flow cytometry

Single cell suspensions in PBS were prepared from the indicated lymphoid organs. Two million cells/sample were blocked with FcR block (2.4G2) 1 μg/ml for 15 min at 4°C and incubated with the indicated antibodies or sema-Fc proteins for 15 minutes at 4°C. After washing with cold PBS (200μl), the cells were spun at 1200rpm for 5min and, when necessary, incubated with streptavidin-APC-Cy7. After another wash with cold PBS, cells were resuspended in PBS and analyzed (FACS Aria, Becton-Dickinson CA).

Confocal microscopy

Frozen thymi embedded in OTC compound (Sakura Finetek, CA) were sliced into 4μm-thick sections and fixed in acetone for 10 min. After rehydration with PBS, the frozen sections were stained with anti-CD69-FITC or ER-TR5 (rat IgM)/anti-rat IgM-Alexafluor647 (Invitrogen, CA), anti-CD8α-TRITC and anti-CD4 (GK1.5)-Alexafluor647. Images were obtained using a Zeiss LSM510 (Ar and He-Ne lasers; excitation at 488nm, 546nm and 633nm) confocal laser-scanning microscope (Carl Zeiss MicroImaging, NY).

Detailed experimental procedures for purification of sema3E-Fc, sema3F-Fc and plexinD1-Fc proteins, measurement of plexinD1-semaphorin interactions using surface plasmon resonance, microarray analysis, laser capture microdissection, migration assay, fetal liver cell transplantation, immunohistochemistry, immunoprecipitation and western blotting are found in supplementary methods.

Statistical analysis

Data are presented as mean values ± one standard error (SE).

Supplementary Material

Refer to Web version on PubMed Central for supplementary material.

Acknowledgements

We acknowledge the excellent technical assistance of Signoretti, Sabina, M.D. and Elizabeth Witten. This work was supported, in part, by National Institutes of Health Grant AI19807 to ELR and AI078340 to LKC.

References

Anderson G, Jenkinson EJ. Lymphostromal interactions in thymic development and function. Nat Rev Immunol 2001;1:31–40. [PubMed: 11905812]

Ansel KM, Cyster JG. Chemokines in lymphopoiesis and lymphoid organ development. Curr Opin Immunol 2001;13:172–179. [PubMed: 11228410]

Campbell JJ, Pan J, Butcher EC. Cutting edge: developmental switches in chemokine responses during T cell maturation. J Immunol 1999;163:2353–2357. [PubMed: 10452965]

DeKoning J, DiMolfetto L, Reilly C, Wei Q, Havran WL, Lo D. Thymic cortical epithelium is sufficient for the development of mature T cells in relB-deficient mice. J Immunol 1997;158:2558–2566. [PubMed: 9058787]

Elewaut D, Ware CF. The unconventional role of LT alpha beta in T cell differentiation. Trends Immunol 2007;28:169–175. [PubMed: 17336158]

Ghendler Y, Hussey RE, Witte T, Mizoguchi E, Clayton LK, Bhan AK, Koyasu S, Chang HC, Reinherz EL. Double-positive T cell receptor(high) thymocytes are resistant to peptide/major histocompatibility complex ligand-induced negative selection. Eur J Immunol 1997;27:2279–2289. [PubMed: 9341770]

Gitler AD, Lu MM, Epstein JA. PlexinD1 and semaphorin signaling are required in endothelial cells for cardiovascular development. Dev Cell 2004;7:107–116. [PubMed: 15239958]

Gu C, Yoshida Y, Livet J, Reimert DV, Mann F, Merte J, Henderson CE, Jessell TM, Kolodkin AL, Ginty DD. Semaphorin 3E and plexin-D1 control vascular pattern independently of neuropilins. Science 2005;307:265–268. [PubMed: 15550623]

Klug DB, Carter C, Crouch E, Roop D, Conti CJ, Richie ER. Interdependence of cortical thymic epithelial cell differentiation and T-lineage commitment. Proc Natl Acad Sci USA 1998;95:11822–11827. [PubMed: 9751749]

Kruger RP, Aurandt J, Guan KL. Semaphorins command cells to move. Nat Rev Mol Cell Biol 2005;6:789–800. [PubMed: 16314868]

Kurobe H, Liu C, Ueno T, Saito F, Ohigashi I, Seach N, Arakaki R, Hayashi Y, Kitagawa T, Lipp M, et al. CCR7-dependent cortex-to-medulla migration of positively selected thymocytes is essential for establishing central tolerance. Immunity 2006;24:165–177. [PubMed: 16473829]

Kutlesa S, Wessels JT, Speiser A, Steiert I, Muller CA, Klein G. E-cadherin-mediated interactions of thymic epithelial cells with CD103+ thymocytes lead to enhanced thymocyte cell proliferation. J Cell Sci 2002;115:4505–4515. [PubMed: 12414996]

Kwan J, Killeen N. CCR7 directs the migration of thymocytes into the thymic medulla. J Immunol 2004;172:3999–4007. [PubMed: 15034011]

Ladi E, Yin X, Chtanova T, Robey EA. Thymic microenvironments for T cell differentiation and selection. Nat Immunol 2006;7:338–343. [PubMed: 16550196]

Lerner A, Clayton LK, Mizoguchi E, Ghendler Y, van Ewijk W, Koyasu S, Bhan AK, Reinherz EL. Cross-linking of T-cell receptors on double-positive thymocytes induces a cytokine-mediated stromal activation process linked to cell death. EMBO J 1996;15:5876–5887. [PubMed: 8918465]

Liu C, Saito F, Liu Z, Lei Y, Uehara S, Love P, Lipp M, Kondo S, Manley N, Takahama Y. Coordination between CCR7- and CCR9-mediated chemokine signals in prevascular fetal thymus colonization. Blood 2006;108:2531–2539. [PubMed: 16809609]

Misslitz A, Pabst O, Hintzen G, Ohl L, Kremmer E, Petrie HT, Forster R. Thymic T cell development and progenitor localization depend on CCR7. J Exp Med 2004;200:481–491. [PubMed: 15302903]

Norment AM, Bogatzki LY, Gantner BN, Bevan MJ. Murine CCR9, a chemokine receptor for thymus-expressed chemokine that is up-regulated following pre-TCR signaling. J Immunol 2000;164:639–648. [PubMed: 10623805]

Plotkin J, Prockop SE, Lepique A, Petrie HT. Critical role for CXCR4 signaling in progenitor localization and T cell differentiation in the postnatal thymus. J Immunol 2003;171:4521–4527. [PubMed: 14568925]

Reichardt HM, Kaestner KH, Tuckermann J, Kretz O, Wessely O, Bock R, Gass P, Schmid W, Herrlich P, Angel P, Schutz G. DNA binding of the glucocorticoid receptor is not essential for survival. Cell 1998;93:531–541. [PubMed: 9604929]

Rodewald HR. Thymus organogenesis. Annu Rev Immunol 2008;26:355–388. [PubMed: 18304000]

Rossi SW, Jenkinson WE, Anderson G, Jenkinson EJ. Clonal analysis reveals a common progenitor for thymic cortical and medullary epithelium. Nature 2006;441:988–991. [PubMed: 16791197]

Schwarz DA, Katayama CD, Hedrick SM. Schlafen, a new family of growth regulatory genes that affect thymocyte development. Immunity 1998;9:657–668. [PubMed: 9846487]

Shibata K, Imarai M, van Bleek GM, Joyce S, Nathenson SG. Vesicular stomatitis virus antigenic octapeptide N52-59 is anchored into the groove of the H-2Kb molecule by the side chains of three amino acids and the main-chain atoms of the amino terminus. Proc Natl Acad Sci U S A 1992;89:3135–3139. [PubMed: 1313583]

Shores EW, Van Ewijk W, Singer A. Maturation of medullary thymic epithelium requires thymocytes expressing fully assembled CD3-TCR complexes. Int Immunol 1994;6:1393–1402. [PubMed: 7819148]

Sun Z, Unutmaz D, Zou YR, Sunshine MJ, Pierani A, Brenner-Morton S, Mebius RE, Littman DR. Requirement for RORgamma in thymocyte survival and lymphoid organ development. Science 2000;288:2369–2373. [PubMed: 10875923]

Surh CD, Ernst B, Sprent J. Growth of epithelial cells in the thymic medulla is under the control of mature T cells. J Exp Med 1992;176:611–616. [PubMed: 1500862]

Suzuki K, Kumanogoh A, Kikutani H. Semaphorins and their receptors in immune cell interactions. Nat Immunol 2008;9:17–23. [PubMed: 18087252]

Swainson L, Kinet S, Manel N, Battini JL, Sitbon M, Taylor N. Glucose transporter 1 expression identifies a population of cycling CD4+ CD8+ human thymocytes with high CXCR4-induced chemotaxis. Proc Natl Acad Sci U S A 2005;102:12867–12872. [PubMed: 16126902]

Toyofuku T, Yabuki M, Kamei J, Kamei M, Makino N, Kumanogoh A, Hori M. Semaphorin-4A, an activator for T-cell-mediated immunity, suppresses angiogenesis via Plexin-D1. EMBO J 2007;26:1373–1384. [PubMed: 17318185]

Turka LA, Schatz DG, Oettinger MA, Chun JJ, Gorka C, Lee K, McCormack WT, Thompson CB. Thymocyte expression of RAG-1 and RAG-2: termination by T cell receptor cross-linking. Science 1991;253:778–781. [PubMed: 1831564]

Uehara S, Song K, Farber JM, Love PE. Characterization of CCR9 expression and CCL25/thymus-expressed chemokine responsiveness during T cell development: CD3(high)CD69+ thymocytes and gammadeltaTCR+ thymocytes preferentially respond to CCL25. J Immunol 2002;168:134–142. [PubMed: 11751956]

Ueno T, Hara K, Willis MS, Malin MA, Hopken UE, Gray DH, Matsushima K, Lipp M, Springer TA, Boyd RL, et al. Role for CCR7 ligands in the emigration of newly generated T lymphocytes from the neonatal thymus. Immunity 2002;16:205–218. [PubMed: 11869682]

Ueno T, Saito F, Gray DH, Kuse S, Hieshima K, Nakano H, Kakiuchi T, Lipp M, Boyd RL, Takahama Y. CCR7 signals are essential for cortex-medulla migration of developing thymocytes. J Exp Med 2004;200:493–505. [PubMed: 15302902]

Vance RE, Kraft JR, Altman JD, Jensen PE, Raulet DH. Mouse CD94/NKG2A is a natural killer cell receptor for the nonclassical major histocompatibility complex (MHC) class I molecule Qa-1(b). J Exp Med 1998;188:1841–1848. [PubMed: 9815261]

Vicari AP, Figueroa DJ, Hedrick JA, Foster JS, Singh KP, Menon S, Copeland NG, Gilbert DJ, Jenkins NA, Bacon KB, et al. TECK: a novel CC chemokine specifically expressed by thymic dendritic cells and potentially involved in T cell development. Immunity 1997;7:291–301. [PubMed: 9285413]

Watakabe A, Ohsawa S, Hashikawa T, Yamamori T. Binding and complementary expression patterns of semaphorin3E and plexinD1 in the mature neocortices of mice and monkeys. J Comp Neurol 2006;499:258–273. [PubMed: 16977617]

Wurbel MA, Philippe JM, Nguyen C, Victorero G, Freeman T, Wooding P, Miazek A, Mattei MG, Malissen M, Jordan BR, et al. The chemokine TECK is expressed by thymic and intestinal epithelial cells and attracts double- and single-positive thymocytes expressing the TECK receptor CCR9. Eur J Immunol 2000;30:262–271. [PubMed: 10602049]

Yamamoto M, Suzuki K, Okuno T, Ogata T, Takegahara N, Takamatsu H, Mizui M, Taniguchi M, Chedotal A, Suto F, et al. Plexin-A4 negatively regulates T lymphocyte responses. Int Immunol 2008;20:413–420. [PubMed: 18209113]

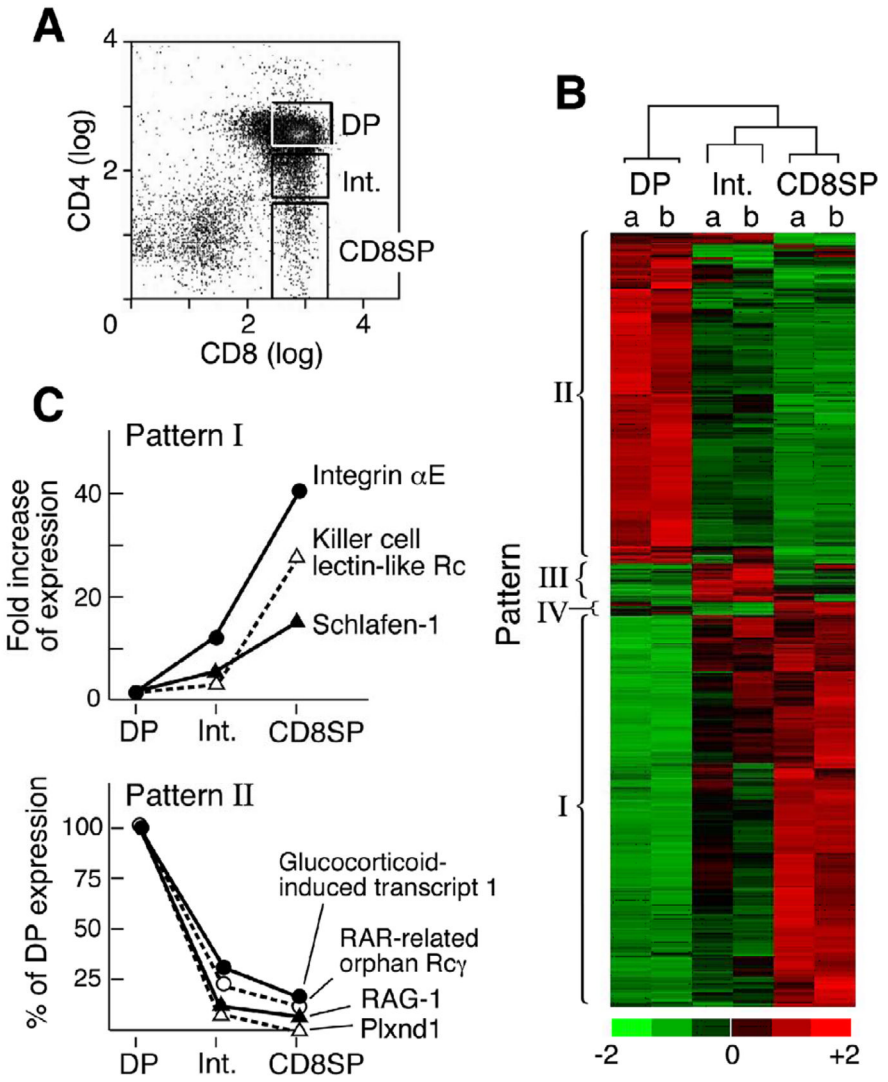

Figure 1. Global expression analysis of DP to CD8 SP development in N15 TCR $tg^{+/+}$ $RAG\text{-}2^{-/-}$ $H\text{-}2^{b}$ mice

A. Thymocytes of N15TCR$tg^{+/+}$ $RAG2^{-/-}$ mice were stained with anti-CD8α-FITC and anti-CD4-PE. Three different populations were sorted based on the CD4 cell surface expression level: DP is $CD8^{high}CD4^{high}$, Int is $CD8^{high}/CD4^{int}$ (intermediate population) and CD8 SP is mature CD8 single positive. Total RNA was isolated from sorted thymocytes and used for microarray analysis as described in the supplementary methods. B. Hierarchical clustering was performed with genes that show significant changes (LCB >2.0). C. Gene expression Patterns I and II as noted in B. The 391 genes showing an increase during maturation were clustered in pattern I. The 328 genes that decreased (LCB <−2.0) with maturation cluster to make up pattern II. R: Receptor. Pattern III and IV are altered in the Int population only and documented in Fig. S1 and http://cvc.dfci.harvard.edu/share_folder/N15RAG-2ko_microarray_data/.

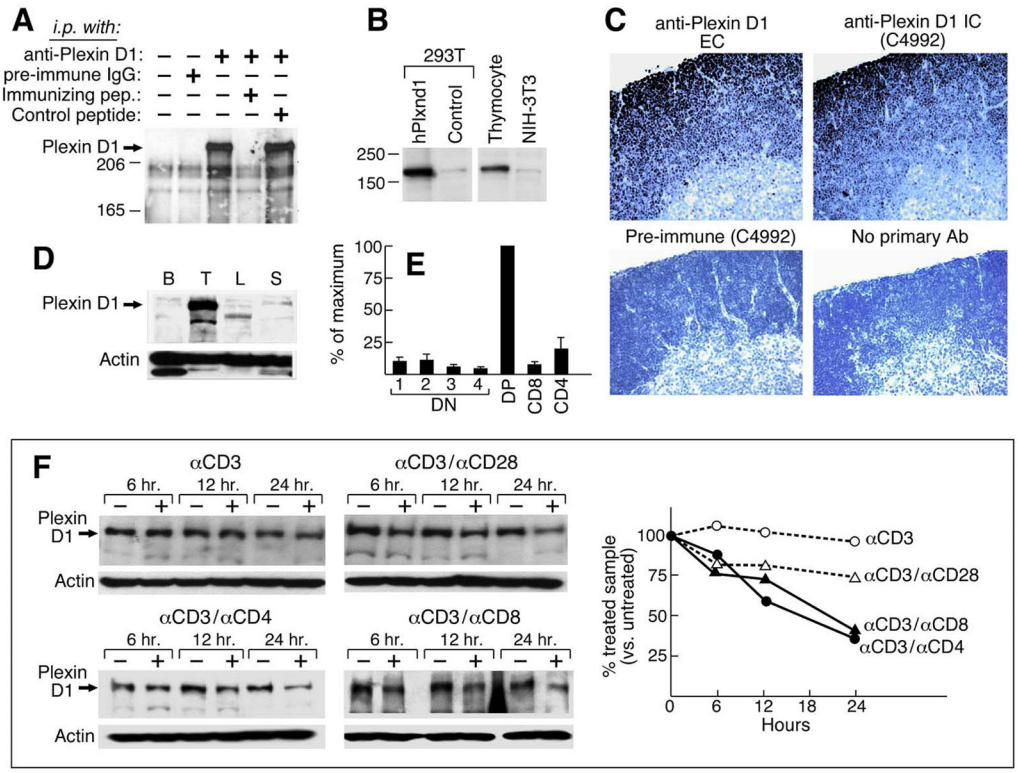

Figure 2. Expression and regulation of plexin D1 on thymocytes

A. A lysate of surface biotinylated thymocytes from 3–4 week old B6 mice was prepared. Following preclearing with goat IgG agarose, samples representing 2×10^7 cells were incubated with preimmune Ab, affinity-purified anti-plexin D1 IC or with the same Ab plus a 150-fold molar excess of the immunizing peptide or an irrelevant control peptide. After SDS/PAGE and transfer, the membrane was probed with steptavidin-HRP. B. Western blotting using affinity-purified anti-plexin D1 IC on lysates of 293T cells transfected with human plexin D1 cDNA, 293-T cells transfected with an irrelevant control cDNA, primary thymocytes, and NIH3T3 mouse fibroblasts separated by SDS-PAGE (8%). C. Paraffin sections were stained with indicated anti-plexin D1 EC, IC or preimmune serum as a control. Sections were counterstained with Mayer's hematoxylin. D. Single cell suspensions were prepared from the indicated organs of C57BL/6 mice. Total cell lysates were resolved on 6% SDS-PAGE and blotted with anti-plexin D1 IC and anti-actin antiserum (B: bone marrow; T: thymus; L: lymph node; S: spleen). E. Total RNAs were isolated from sorted thymocyte populations and used for cDNA synthesis. Synthesized cDNA was used for Realtime PCR analysis according to the manufacturer's instructions (ABI). Normalized values using GAPDH real time PCR values with the same cDNA as a control were converted to % of maximum value (value of DP thymocyte population). Error bars are the standard error of 3 independent experiments. F. Single cell suspensions of B6 thymocytes were prepared and then stimulated with the indicated combinations of mAbs for 6, 12 and 24 h. Total cell extracts were prepared from stimulated cells after removal of dead cells using Histopaq (Sigma, MO) and analyzed by western blot with anti-plexin D1 IC. This figure is representative of 3 independent experiments. The graph shows quantitated-plexin D1 band intensities normalized as % of untreated sample.

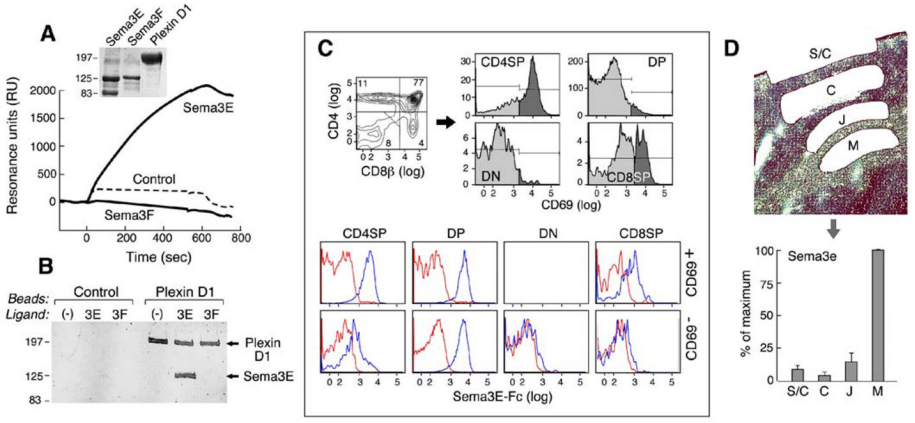

Figure 3. Sema3E-Fc binds the plexinD1 ectodomain

A. Purified plexinD1 ectodomain (plexin D1-Fc), sema3E (sema3E-Fc) and sema3F (sema3F-Fc) proteins were analyzed by Coomassie brilliant blue staining after being resolved by SDS-PAGE. The interaction of plexinD1-Fc and sema-Fc proteins was analyzed using BIAcore as described in supplementary methods. B. PlexinD1-Fc was conjugated to UltraLink Biosupport (Pierce, NJ). Sema3E-Fc and sema3F-Fc were incubated with crosslinked plexinD1-Fc. After washing, proteins were eluted by boiling in protein sample buffer and analyzed by Coomassie brilliant blue staining after resolution on SDS-PAGE. Control is unconjugated UltraLink Biosupport resin. 3E is sema3E-Fc and 3F is sema3F-Fc as a negative control. C. Total thymocytes were stained for CD4, CD8β and CD69. The upper left panel shows the CD4/CD8β pattern and the numbers on gated regions are % of total thymocytes. The upper right histograms show the expression of CD69 in the indicated subpopulations. The darker gray area of the histogram is CD69 staining and the light gray indicates control antibody staining. Lower panels show $CD69^{-}$ and $CD69^{+}$ thymocytes stained with purified sema3E-Fc (10μg/ml)(blue) or Fc-only protein (red) developed with anti-mouse IgG_{2c}-PE. The fluorescence of sema3E-Fc is plotted in the indicated thymocyte populations. The numbers on gated regions are % of total thymocytes. The histogram for $CD69^{+}$ DN cells are omitted because of the low cell number. D. Indicated regions were collected as described in Experimental Procedures. Total RNAs were isolated and used for cDNA synthesis. Real time PCR was performed as described in Fig 2E. Error bar is standard error of 4 independent experiments. S/C: subcapsullary zone and thymic capsule; C: Cortex; J: corticomedullary junction; M: medulla.

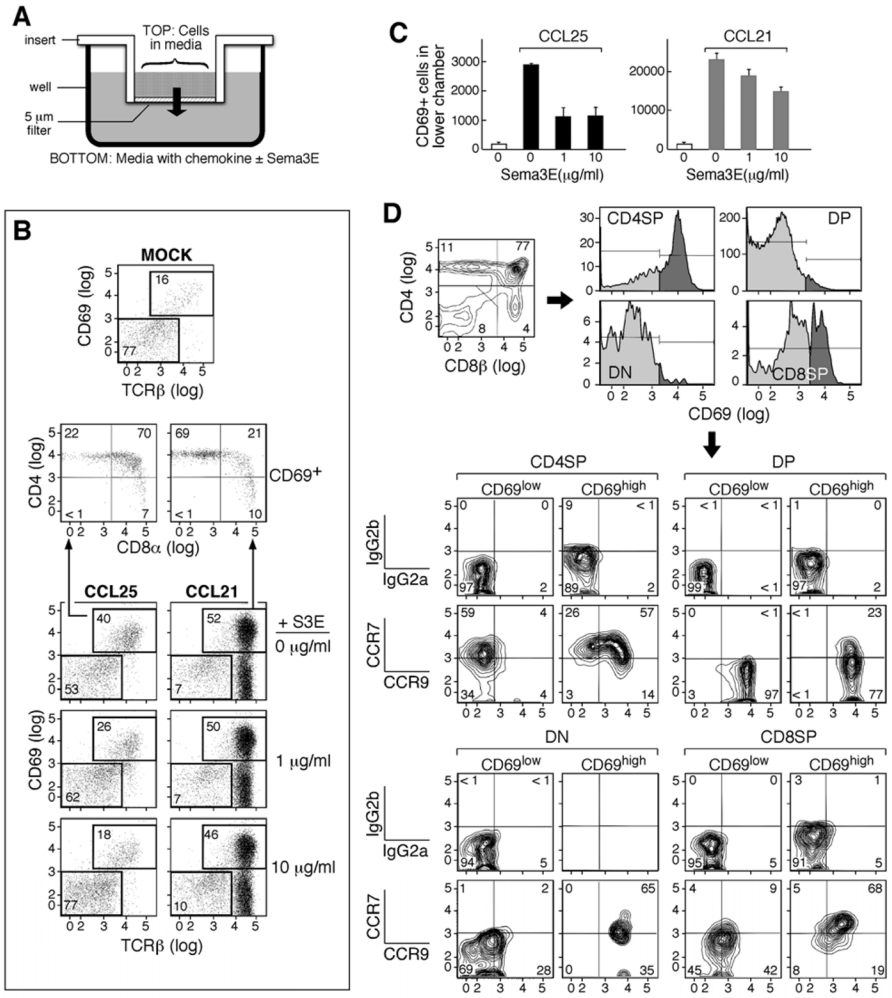

Figure 4. Inhibition of chemokine-mediated migration by sema3E-Fc

A. Migration assays were performed in 24-well transwell plates with a 5μm pore size as depicted. Cells were added to the insert and the indicated chemokines were added to the bottom well with purified sema3E-Fc or Fc-only protein. B. After 2 hrs, cells that had migrated to the bottom well were harvested and stained with anti-CD4, anti-CD8α, anti-CD69, and anti-TCRβ mAbs. Mock in the top panel is a sample without chemokine treatment. CCL25 was added to the bottom well in the left set of panels and CCL21 to the right set. The concentration of S3E (sema3E-Fc) is indicated on the right of each panel. In the middle panels, the CD4/CD8 patterns of the $CD69^+$ cells that migrated to the bottom of the well are shown for the CCL25- and CCL21-treated cultures. More than two-thirds of $CD69^+$ thymocytes were DP in CCL25-treated and less than one-quarter were DP in CCL21-treated cultures. C. An aliquot of cells harvested from B was counted and the number of $CD69^+$ thymocytes migrating in response to CCL25 or CCL21 in the presence of various concentrations of sema3E was determined. Error bars are the standard error of one triplicate experiment. D. Single cell suspensions were prepared from B6 thymus, stained with the indicated mAbs and analyzed on a flowcytometer. Data were analyzed using FlowJo (TreeStar, Or). The upper left panel is a CD4/CD8 profile. CD69 expression in each gated population is depicted with dark gray above control staining in the upper right panels. In the lower four sets of panels, CCR7 and CCR9 expression in each population (gated on CD69, CD4 and CD8 expression) are shown. The upper row in each set of four shows samples stained with isotype control mAbs while the lower row shows those

stained with anti-CCR7 and anti-CCR9 mAbs. The numbers in the panels are % of gated populations.

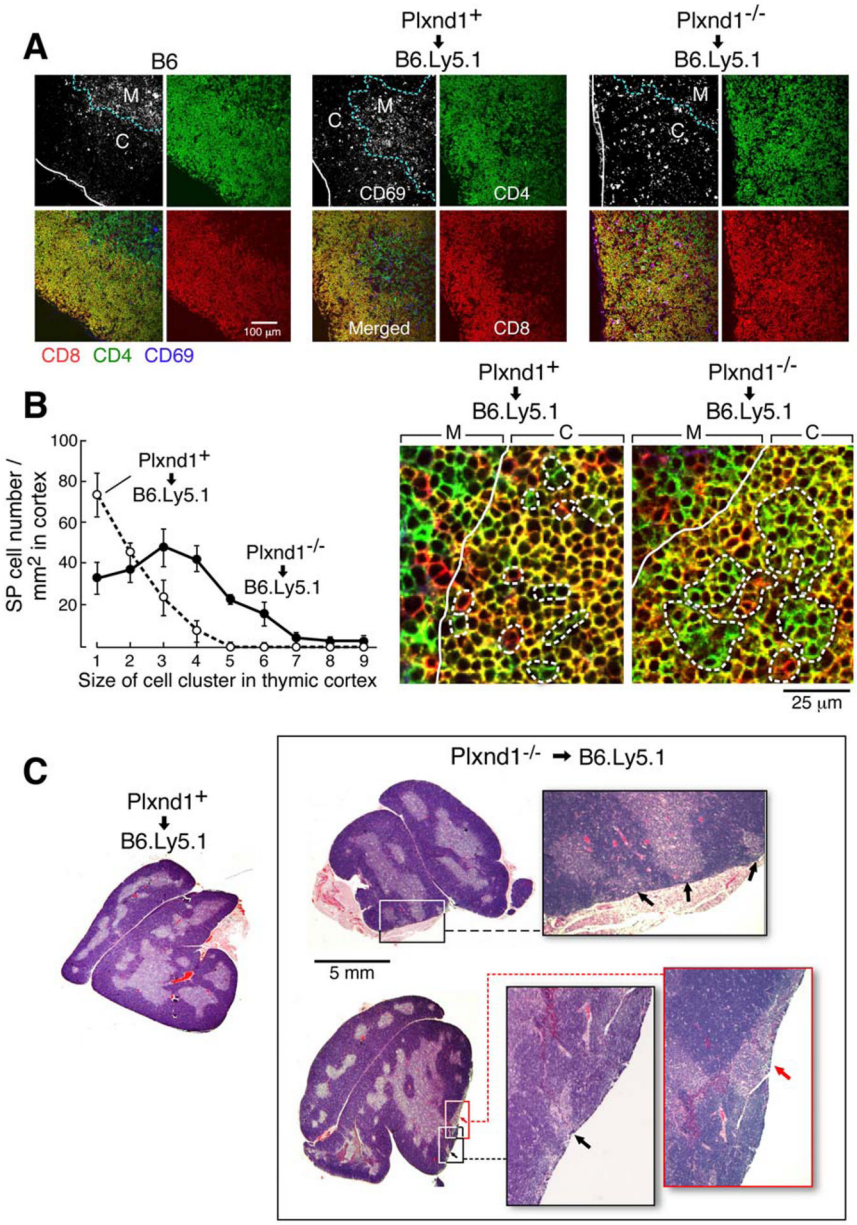

Figure 5. Aberrations in localization of CD69$^+$ thymocytes and medullary structure in Plxnd1$^{-/-}$ fetal liver cell transplanted thymus

A. Cryosections of reconstituted mice were stained with anti-CD4/CD8α/CD69 mAbs. Stained sections were analyzed using a Carl Zeiss LSM510 confocal microscope. The blue dashed line follows the corticomedullary junction and solid white line shows the thymic capsule. This figure is representative of four independent transplantation experiments. CD69 is depicted as white spots in the upper left section of each quartet and as blue spots in the merged image in the lower left section of the same quartet. CD4 is green and CD8 is red. (Note that CD69$^+$ cells co-expressing CD4 and/or CD8 appear in different colors.) The sections are from B6 mice, mice reconstituted with *Plxnd1*$^+$ or *Plxnd1*$^{-/-}$ fetal liver cells (left, middle and right panels, respectively). Cryosections were stained with anti CD4 (Green)/CD8α (Red)/ER-TR5 (Blue; a marker of mTEC) mAbs. B. Stained sections were analyzed as described in A and represent magnified images of inserts (a) and (b) shown in Fig. S6A. The solid line is the corticomedullary

junction and the dashed line is the boundary of SP thymocytes. The graph depicts the distribution of SP thymocytes in the cortex (ER-TR5^{-} area), analyzed by plotting SP thymocyte numbers based on the size of SP thymocyte clusters in the cortex. SP thymocyte clusters and number of cells per cluster were counted from 5 different slides. The error bar is the standard error. C. Medullary structures were visualized by staining paraffin sections of transplanted mice with hematoxylin and eosin. The indicated inserts in the chimeric thymi from *Plxnd1*$^{-/-}$ fetal liver cell donors are magnified and the arrows highlight contact between the medulla and the thymic capsule.

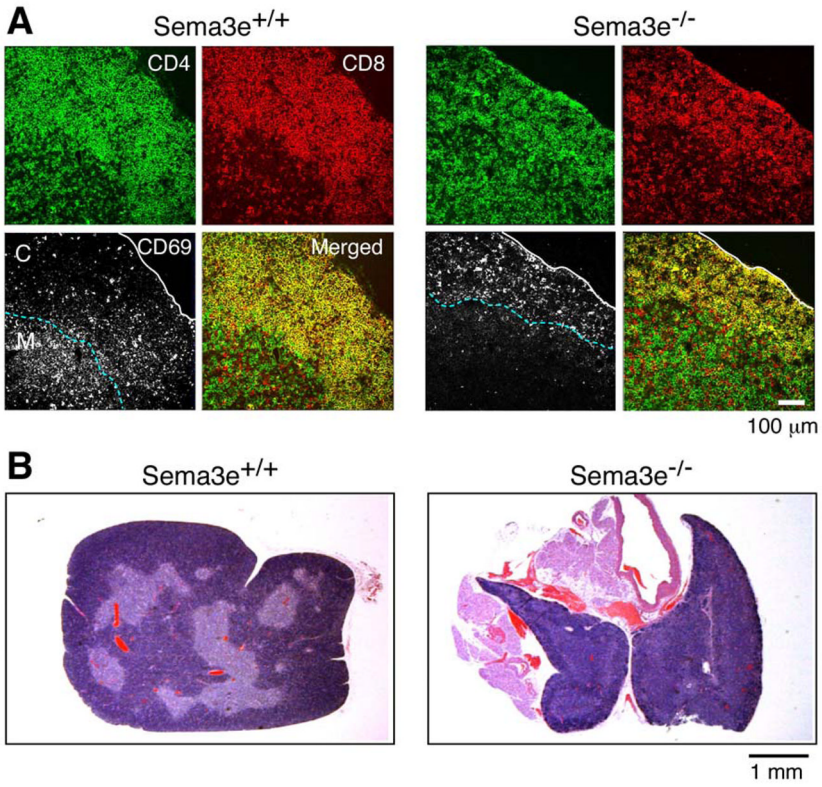

Figure 6. Aberrations in localization of CD69^{+} thymocytes and corticomedullary structure in Sema3e$^{-/-}$ thymus

A. Cryosections were stained as described in Fig. 5A. The blue dashed line follows the corticomedullary junction and the solid white line outlines the thymic capsule. This figure is representative of three independent analyses. CD69 is depicted as the white signal in the lower left section of each quartet. CD4 is green and CD8 is red. The sections are from *Sema3e*$^{-/-}$ mice and *Sema3e*$^{+/+}$ littermate controls. White scale bar = 100μm. B. Medullary structures from *Sema3e*$^{-/-}$ mice and *Sema3e*$^{+/+}$ littermate controls were visualized by staining paraffin sections with hematoxylin and eosin. Scale bar = 1mm.

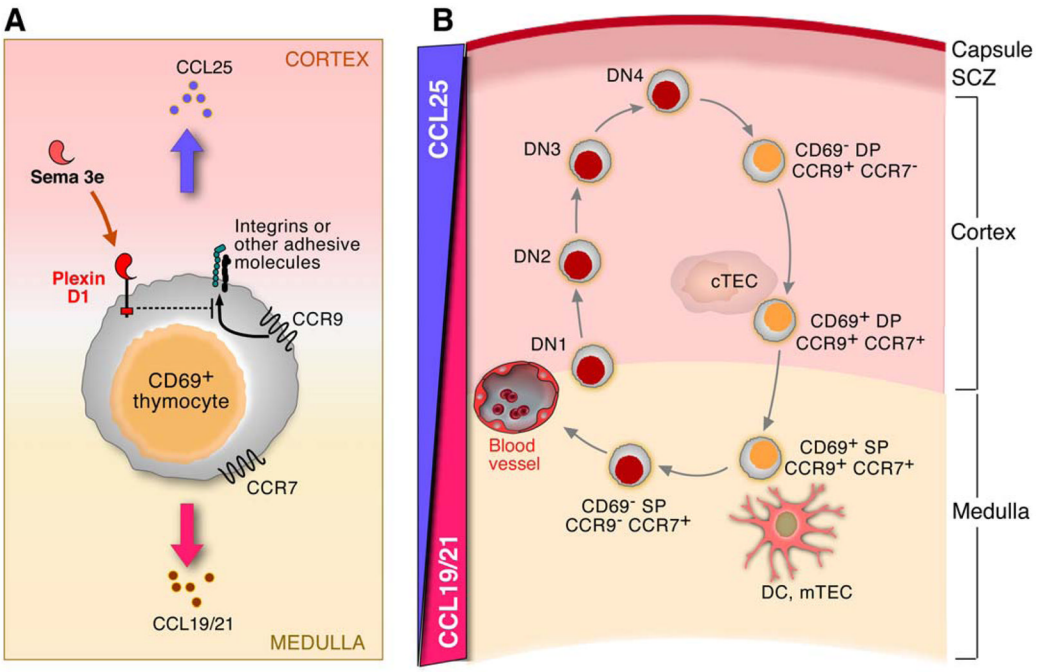

Figure 7. Model of plexin D1 function in intrathymic migration

A. Plexin D1 inhibits CCR9 signaling in activated CD69$^+$ DP thymocytes. As described in the text, this inhibition is selective for CCR9 and probably linked with other adhesion molecules. B. Because plexinD1 inhibits migration signals mediated through CCR9 via CCL25, activated CD69$^+$ DP thymocytes rapidly migrate toward the medulla in response to CCL19/21 rather than responding to the influence of CCL25 in the cortex. Yellow cells are plexinD1$^+$ thymocytes; red cells are plexinD1$^-$ thymocytes; DC are dendritic cells; mTEC are medullary thymic epithelial cells; cTEC are cortical thymic epithelial cells. SCZ: subcapsular zone. For simplicity, death by neglect of CD69$^-$ thymocytes or by negative selection of CD69$^+$ thymocytes has been omitted.